Eurographics/ IEEE-VGTC Symposium on Visualization (2007)
Ken Museth, Torsten Möller, and Anders Ynnerman (Editors)

Functional Unit Maps for Data-Driven Visualization of High-Density EEG Coherence

Michael ten Caat[1,2], Natasha M. Maurits[2,3], and Jos B. T. M. Roerdink[1,2]

[1]Institute for Mathematics and Computing Science, University of Groningen, The Netherlands
[2]BCN Neuroimaging Center, University of Groningen, The Netherlands
[3]Department of Neurology, University Medical Center Groningen, University of Groningen, The Netherlands

Abstract

Synchronous electrical activity in different brain regions is generally assumed to imply functional relationships between these regions. A measure for this synchrony is electroencephalography (EEG) coherence, computed between pairs of signals as a function of frequency. Existing high-density EEG coherence visualizations are generally either hypothesis-driven, or data-driven graph visualizations which are cluttered. In this paper, a new method is presented for data-driven visualization of high-density EEG coherence, which strongly reduces clutter and is referred to as functional unit (FU) map. Starting from an initial graph, with vertices representing electrodes and edges representing significant coherences between electrode signals, we define an FU as a set of electrodes represented by a clique consisting of spatially connected vertices. In an FU map, the spatial relationship between electrodes is preserved, and all electrodes in one FU are assigned an identical gray value. Adjacent FUs are visualized with different gray values and FUs are connected by a line if the average coherence between FUs exceeds a threshold. Results obtained with our visualization are in accordance with known electrophysiological findings. FU maps can be used as a preprocessing step for conventional analysis.

Categories and Subject Descriptors (according to ACM CCS): E.1 [Data]: Graphs and networks; J.3 [Life and Medical Sciences]: Health

1. Introduction

EEG measures the electrical activity of the brain using electrodes attached to the scalp at multiple locations. Synchronous electrical activity in different brain regions is generally assumed to imply functional relationships between these regions. A measure for this synchrony is electroencephalography (EEG) coherence [MSvdHdJ06], calculated between pairs of electrode signals as a function of frequency. For the analysis of high-density EEG coherence, EEG researchers often employ a hypothesis-driven definition of certain regions of interest (ROIs) in which all electrodes are assumed to record similar signals because of volume conduction effects [HF77, LRMV99]. As an alternative, we introduce an approach for the determination of data-driven ROIs.

Visualization of high-density EEG (at least 64 electrodes) is not always managed well [tCMR05, tCMR07]. A typical visualization of EEG coherence is a two-dimensional graph (layout) with vertices representing electrodes and edges representing significant coherences between electrode signals. Vertices are commonly visualized as dots, edges as lines. For high-density EEG, this graph suffers from the potentially large number of overlapping edges, resulting in a cluttered visualization, e.g., [KBS97,SRSP99]. One common solution to reduce clutter in graph visualizations involves the reorganization of vertex positions [FR91]. However, in our case this is not appropriate, because the electrodes have meaningful positions. Other solutions reorganize edges [WCG03], or vary visual attributes of the edges [HMM00, WCG03]. Existing EEG analyses of high-density EEG are hypothesis-driven, choosing a regularly distributed subset of electrodes, e.g., [MSvdHdJ06]. Different approaches employ a contingency table with electrodes along the rows and columns [KBS97], or first localize dipoles corresponding to maximally independent components in the data, and then calculate coherence between dipole activities [DMFTS02].

As an alternative to the hypothesis-driven approach, we

here propose a data-driven visualization of high-density coherence, which strongly reduces clutter and is referred to as functional unit (FU) map. It obtains data-driven ROIs, referred to as FUs, which are spatially connected sets of electrodes recording pairwise significantly coherent signals. In an initial graph, vertices are mapped to a two-dimensional image maintaining the spatial relations between electrode positions. Significant coherences between pairs of electrode signals are represented by edges between corresponding vertices. In this initial graph, an FU is represented by a spatially connected clique. A clique is a vertex set in which every two-element subset is connected by an edge. The spatial connectedness of vertices is determined by a Voronoi diagram [Vor08] of the electrode positions.

The detection of FUs is based on maximal clique detection [BK73], which we extend to find sets of spatially connected vertices. The FU map displays all electrodes belonging to one FU with the same color. If the average coherence between two FUs exceeds a significance threshold, a line is drawn between the corresponding FU centers.

Our method bears similarity to that of Gladwin et al. [GLdJ06], showing connecting lines between clusters. Whereas they use a hypothesis-driven approach to determine the number of clusters and the location of the clusters, our method uses a fully data-driven approach.

We illustrate FU maps for different datasets and different parameters. Results are related to conventional findings.

2. EEG Data

During an EEG experiment, the electrical activity of the brain is measured using up to 512 electrodes attached to the scalp at different locations. To reduce impedance, a conductive gel is applied between skin and electrodes, which are often held in fixed positions by an elastic cap. Each electrode carries a unique labeling by a combination of letters and digits (e.g., F3, Cz, P4, as in Fig. 1, right). From all electrodes simultaneously, the electrical potential is measured at sampling rates typically up to 2000 Hz. The measured signal from each electrode is amplified, resulting in one recording channel for every electrode. If there are many electrodes, the term 'multichannel' or 'high-density' EEG is used.

Activity from one source can result in a strong signal recorded by multiple electrodes, as a result of *volume conduction* [HF77]. Therefore, nearby electrodes usually record similar signals. Often, there are several sources of activity at different locations. These sources can be synchronous. Consequently, signals recorded by electrodes that are far apart can also be similar. Coherence is a measure for the similarity of signals as a function of frequency. The coherence c as a function of frequency λ for two continuous time signals x and y is defined as the absolute square of the cross-spectrum f_{xy} normalized by the autospectra f_{xx} and f_{yy} [HRA*95], having values in the interval $[0,1]$: $c_\lambda(x,y) = \frac{|f_{xy}(\lambda)|^2}{f_{xx}(\lambda) f_{yy}(\lambda)}$. An event-related potential (ERP) is an EEG recording of the brain response to a sensory stimulus. For L repetitive stimuli, the EEG data can be separated into L segments, each containing one ERP. A *significance threshold* for the estimated coherence is then given by [HRA*95]

$$\theta = 1 - p^{1/(L-1)}, \tag{1}$$

where p is a probability value associated with a confidence level α, such that $p = 1 - \alpha$. Throughout this paper, we use $p = 0.05$, unless stated otherwise.

3. Related Work

3.1. Graph Theory

Most coherence representations use graph visualizations. A graph $G = (V,E)$ consists of a set of vertices V and a set of edges $E \subseteq V \times V$. The vertices u and v are called neighbors or adjacent if there is one edge between them. The neighborhood of vertex v is the collection of all neighbors of v. In a directed graph, the set E consists of ordered pairs of vertices from V. In an undirected graph, the pairs are not ordered. A directed edge is denoted as $e = (u,v)$, an undirected edge as $e = \{u,v\}$; u and v are called incident with e, and e is said to be incident with u and v. The degree of a vertex is the number of edges incident with this vertex. A plane graph is a graph without intersecting edges in the two-dimensional plane. A walk between two vertices is a sequence of edges $(e_1,...,e_n)$, with vertices $v_0,...,v_n$ such that $e_i = \{v_{i-1},v_i\}$. If a walk exists between two vertices, they are called connected. If an edge $e = \{v,v\}$ exists, the vertex v is called self-connected. For a graph $G = (V,E)$ and $V' \subseteq V$, the set of all edges with both vertices in V' is denoted as $E|V'$. The graph $G' = (V',E|V')$ is called the (vertex-) induced subgraph on V'. If $V' \subset V$ and $E' \subset E|V'$, then $G' = (V',E')$ is called a subgraph. If any two vertices in $G = (V,E)$ are connected, G is called a connected graph. A maximal connected subgraph of G is a connected component. If all two-element subsets of V are edges, then $G = (V,E)$ is a complete graph. A clique is a set $V' \subseteq V$ such that the induced subgraph on V' is a complete graph. A maximal clique is a clique which is not a subgraph of a larger clique. For a more extensive overview of graph theory, see e.g., Jungnickel [Jun99].

3.2. Graph Visualization

A straightforward graph visualization of EEG coherence represents electrodes as vertices and significant coherences as edges, with vertices shown as dots and edges as lines. In graph layouts of EEG coherence, edge densities can be so high that individual edges cannot be distinguished, and edges can obscure vertices and other visual information, e.g., [KBS97]. Multiple solutions exist to reduce such cluttering of edges.

First, the layout of the vertices can be changed, e.g.,

by using a force-directed placement [FR91]. However, for EEG applications we prefer to maintain the spatial relationship between the vertices representing electrodes. Other solutions vary visual attributes of edges, such as transparency [WCG03], or color, saturation, and line width [HMM00]. However, there can still be many overlapping edges that obscure other visualization elements. Also, the superposition of differently colored lines might result in an undesired mix of colors. Additionally, the layout of the edges can be manipulated, e.g., by interactively curving away edges from the focus of attention [WCG03]. This has the undesirable side-effect that, in an already crowded field of view, the area which is out of focus will be even more crowded. Finally, elements (such as edges) can be left out selectively [CJM03].

3.3. EEG Coherence Visualization

Most EEG analyses of EEG coherence make a hypothesis-driven selection of electrodes, e.g., [MSvdHdJ06]. Only a few data-driven methods are available for the visualization of EEG coherence, and they are suitable for relatively low numbers of edges. One method visualizes coherence for 21 electrodes and all possible electrode combinations, setting out the electrodes along both the rows and columns of a matrix as a tiled display [KBS97]. The result is a square contingency table showing coherence values for all possible electrode pairs. Each table entry is a square in which coherence is displayed between the two corresponding electrode signals as a function of frequency. By arranging the electrodes along the rows and the columns of the matrix, the spatial relations are lost. As a result, consecutive entries in the table do not need to imply coherence between pairs of signals recorded at adjacent electrodes on the scalp.

Other data-driven EEG coherence visualization methods employ graph visualization techniques. Electrodes are commonly shown as dots or circles distributed over a two-dimensional or three-dimensional head shape, while significant coherences are indicated by lines or arrows, e.g., [KBS97, SRSP99]. Especially for high-density EEG with up to 512 vertices, many overlapping edges are possible, resulting in visual clutter.

A different approach uses EEG source analysis to obtain dipole sources. The number of dipole sources is considerably smaller than the number of electrodes. The coherence between dipole source activities can be shown with sources as vertices [DMFTS02]. Despite the low number of vertices, there may still be various overlapping edges. Moreover, there are generally several different but plausible dipole source solutions [Sri99].

Another solution is to cluster the electrodes as described in [GLdJ06]. From a total collection of 128 electrodes, a subselection is made of 66 electrodes. From this subselection, twelve regularly distributed electrodes are chosen as anchors. Each of the remaining electrodes is assigned to the anchor that recorded the most similar signal, provided that the similarity exceeds some significance threshold. The cluster centers are defined as the average of the positions of the electrodes within each cluster. If the similarity calculated between two clusters exceeds a threshold, a line is drawn between the two cluster centers. The main disadvantage of this method is the hypothesis-driven selection of the number of anchors and their positions.

4. Data Representation

4.1. EEG Coherence Data

Data were used from a so-called P300 experiment. During this experiment each participant was instructed to respond to an infrequent auditory target stimulus. The participant counted target tones of 2000 Hz (probability 0.15), alternated with standard tones of 1000 Hz (probability 0.85) which were to be ignored. After the experiment, the participant had to report the number of perceived target tones. The participants studied here were three young adults. The brain response was recorded using an EEG cap with 119 electrodes attached to the scalp. The data were resampled from 1000 Hz to 256 Hz. Each dataset consisted of brain reactions to 20 target tones, recorded in $L = 20$ segments.

A procedure from Neurospec (`www.neurospec.org`) was adopted to compute the coherence. Frequencies between 1 and 30 Hz are typically studied clinically. We calculated the coherence within a low (1-3 Hz) and a high (13-20 Hz) frequency band, because EEG synchrony behaves differently for low and high frequencies [MSvdHdJ06, NSW*97]. The coherence for a frequency band a-b Hz was calculated as the average of the coherence between frequencies a Hz and b Hz. For 119 electrodes, in total 7021 coherence values were computed per frequency (band). If the conductive gel accidentally connected two adjacent electrodes, very high coherences were measured. Coherences higher than 0.99 were therefore ignored.

4.2. Initial Graph

In an (undirected) *initial graph*, vertices represent electrodes and edges represent significant coherences (Eqn. 1) between electrode signals. Vertices are visualized as dots and edges as lines (Fig. 1, left). Vertices are not self-connected. A histogram gives an example of computed coherence values (Fig. 1, middle).

4.3. Voronoi Relationship

To determine spatial relationships between electrodes, a Voronoi diagram [Vor08] is employed which partitions the plane into cells with the same nearest vertex. For EEG data, the vertex set equals the set of electrode positions (Fig. 1).

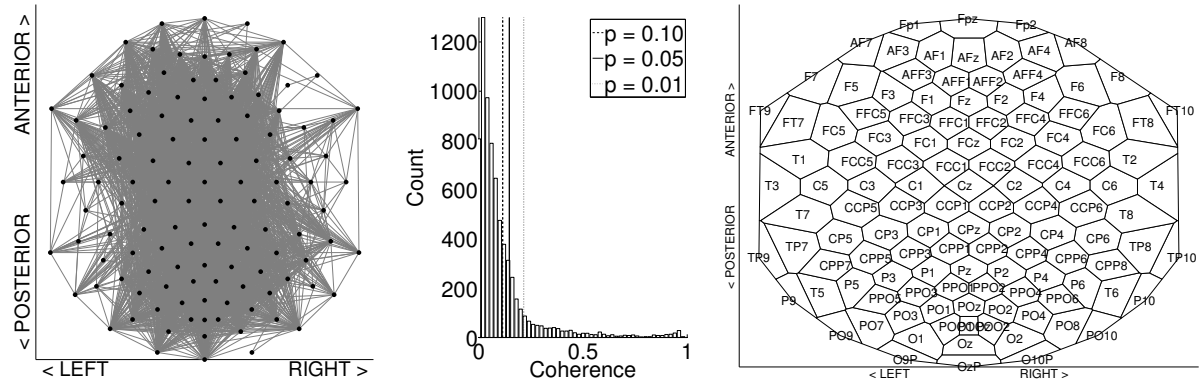

Figure 1: ***Left:*** *Initial graph (EEG frequency band* 1-3 *Hz, dataset* 1*). Vertices represent electrodes, edges represent significant coherences between electrode signals. Edges are visualized as gray lines, vertices as black dots on top of the edges. This corresponds to a common existing data-driven visualization, showing cluttered edges.* ***Middle:*** *Histogram of the corresponding coherence. Vertical lines (dash, solid, dot) indicate significance thresholds associated with three probability levels (*$p = 0.10, 0.05, 0.01$*, respectively).* ***Right:*** *Voronoi diagram with electrode labels in the corresponding cells, having the convex hull of all electrodes as a boundary. To improve the readability, the Voronoi diagram is stretched horizontally. Because the coherence computation is independent of distance, distances between electrodes do not need to be preserved. However, spatial relationships between electrodes are maintained.*

The vertices are referred to as (Voronoi) centers, the boundaries as (Voronoi) polygons. The area enclosed by a polygon is called a (Voronoi) cell. A cell encloses all points which are closest to the center in that particular cell. We call two cells *Voronoi neighbors* if they have a boundary in common. A collection of cells C is called Voronoi-connected if for a pair $\phi_0, \phi_n \in C$ there is a sequence $\phi_0, \phi_1, ..., \phi_n$ of cells in C with each pair ϕ_{i-1}, ϕ_i consisting of Voronoi neighbors. We use the terms "Voronoi neighbor" and "Voronoi-connected" interchangeably for cells, vertices, and electrodes.

5. Functional Unit Maps

Using a hypothesis-driven approach, EEG researchers often define certain regions of interest (ROIs) to analyze high-density EEG coherence. From each ROI, typically one electrode is selected as a marker. Usually, there are about ten to twenty markers. These markers are assumed to record signals that are representative for all electrodes in the corresponding ROI, because of volume conduction effects [HF77]. Instead, we introduce a method to determine a data-driven ROI, called functional unit (FU), which is represented in the initial graph by a clique consisting of a set of spatially connected vertices. Consequently, an FU corresponds to a set of electrodes in which the electrodes record pairwise significantly coherent signals.

5.1. Maximal Cliques

Bron and Kerbosch [BK73] developed a method to detect all maximal cliques in a graph. It first branches the problem, and bounds unsuccessful branches. Its recursive procedure maintains three dynamic vertex sets:

- the set `compsub` contains an increasing or decreasing clique;
- the set `candidates` contains vertices that are connected to all vertices in `compsub` and that can be added to `compsub`;
- the set `not` contains vertices that are connected to all vertices in `compsub` and that have already been added to `compsub` previously.

At each call of the procedure, the first element of `candidates`, say vertex v, is added to `compsub` and removed from `candidates`. Next, `newcandidates` is the intersection of `candidates` and the neighborhood of v. Similarly, `newnot` is the intersection of `not` and the neighborhood of v. If both `newcandidates` and `newnot` are empty, `compsub` contains a maximal clique. This procedure is repeated recursively with local sets `newcandidates` and `newnot`, until the candidate set is empty. In case the procedure is not repeated with `newcandidates` and `newnot`, the vertex most recently added to `compsub` (vertex v) is removed from `compsub` and added to `not`. If any vertex in `newnot` is connected to all vertices in `newcandidates`, then it is known that this vertex will never be removed from `not` and this branch is bounded.

An alternative selection of vertex v is more efficient if there is a large number of overlapping cliques [BK73]. From the set `candidates`, the vertex v^* is selected that has the largest number of connections with the other vertices in `candidates`. If there are more such vertices, then one of

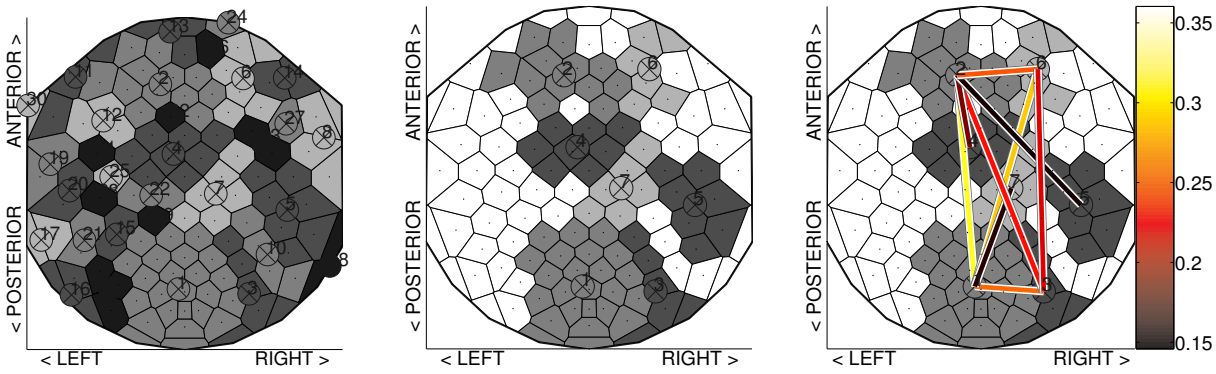

Figure 2: *Functional Unit map (EEG frequency band* 1-3 *Hz, dataset* 1*). **Left:** A circle with a cross inside indicates the geographic center of all Voronoi centers belonging to one FU and has a corresponding gray value. The geographic center can be located in a cell not belonging to the corresponding FU. **Middle:** The same FU map, but with seven FUs larger than* 5 *cells. White Voronoi cells are part of smaller FUs. **Right:** Lines connect FU centers, if the inter-FU coherence exceeds the significance threshold (Eqn. 1). The color of the line depends on the inter-FU coherence (see color bar, with minimum corresponding to the coherence threshold* ≈ 0.15*).*

these is randomly selected. Further, it is assured that v^* is not connected to the vertex just added to `not`. The worst-case time complexity of this alternative is $O(3^{n/3})$, with n the number of vertices, because $3^{n/3}$ is the highest number of cliques [TTT06].

5.2. Voronoi-Connected Maximal Cliques

We extend the method by [BK73] such that it only detects maximal cliques consisting of Voronoi-connected vertices. The three dynamic vertex sets are maintained, but the set `candidates` is split into a set `currentcand` and a set `complcand`.

- The set `currentcand` contains the candidates that are Voronoi neighbor of at least one element in `compsub`; only these can be added to `compsub` at the current step.
- The set `complcand` is the complement of `currentcand` in `candidates`.

Similar to the second version of [BK73], at each call the element from `currentcand` is taken which has the largest number of connections with the other candidates (`currentcand` and `complcand`). Let this element be v'. The set `newcurrentcand` is the intersection of `currentcand` and the Voronoi neighbors of v', united with the Voronoi-neighbors of v' in `complcand`. Consequently, `newcomplcand` consists of the vertices in `complcand` minus the Voronoi neighbors of v'. This is repeated until `newcurrentcand` and `newnot` are empty. The set `(new)not` is maintained as before. This modified procedure results directly in the collection of all Voronoi-connected maximal cliques.

5.3. FU Labeling

Each vertex can be part of more than one (Voronoi-connected) maximal clique. To assign a unique label to every vertex, the following labeling procedure is applied.

First, we define the quantity *total strength* S for an undirected (sub)graph $G = (V,E)$ as the sum of all edge values:

$$S(G) = \sum_{i,j} \{c(v_i,v_j) \mid v_i,v_j \in V : j > i\}. \qquad (2)$$

This value is not normalized for the size of E. Consequently, if two graphs have an equal average coherence, the graph with the larger size has the higher total strength.

The Voronoi-connected maximal cliques are sorted by their total strength, from high to low. The vertex set corresponding to the one with the highest total strength is labeled W_1. The vertices in W_1 are assigned the label 1 and are removed from the remaining (maximal) cliques. If the remaining cliques are not Voronoi-connected any more, they are split into Voronoi-connected components. For every changed clique the total strength is recomputed, and the clique is inserted in an appropriate location in the sorted list of cliques. This procedure is repeated, until all vertices received a label, or until all maximal cliques have been considered. This results in vertex sets labeled $W_1,\ldots,W_M$. Every vertex set W_i ($i \in \{1,2,\ldots,M\}$) is considered to be a functional unit, being a clique consisting of Voronoi-connected vertices.

5.4. FU Map Coloring

Each FU is visualized as a set of identically colored Voronoi cells. Adjacent FUs are colored differently. We call this visualization an *FU map*. The problem of coloring the FUs cor-

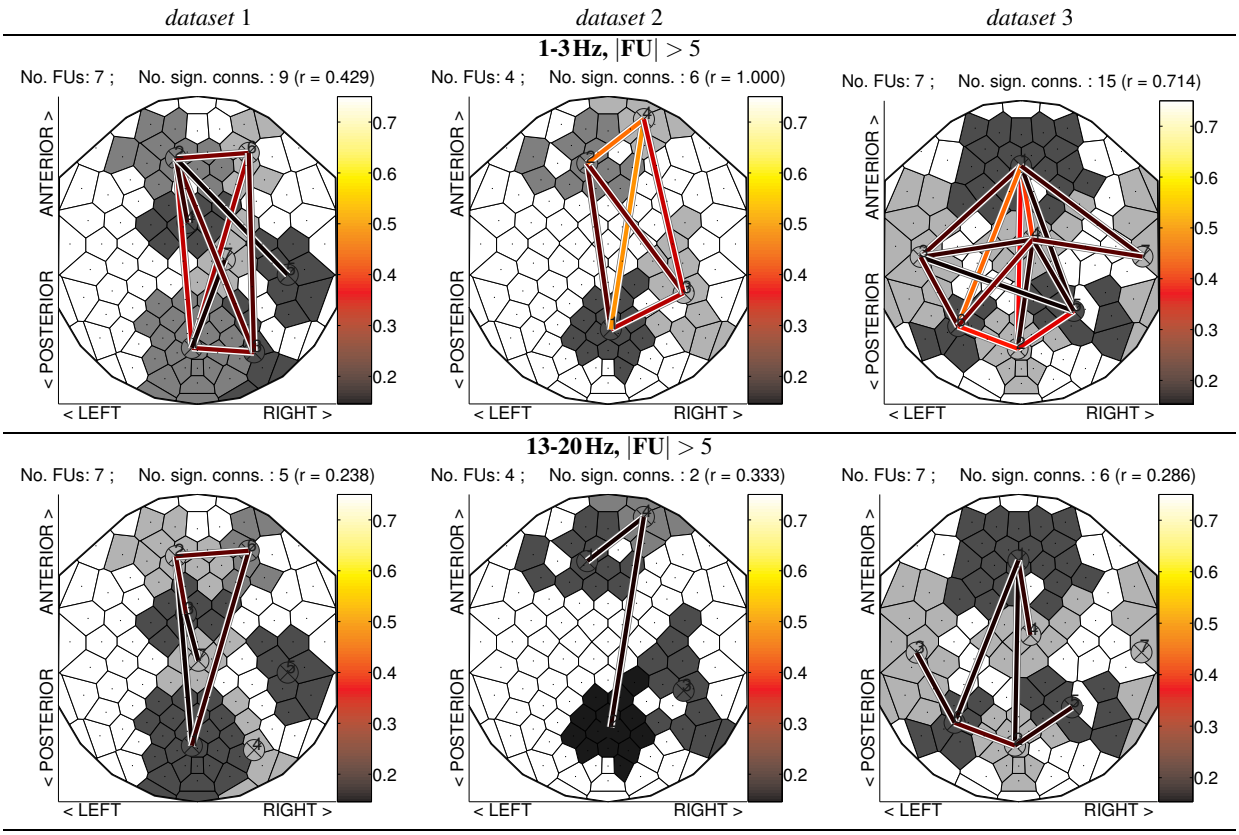

Figure 3: *FU maps with FUs larger than* 5 *cells, for the* 1-3 *Hz EEG frequency band (**top row**) and for* 13-20 *Hz (**bottom row**), for three datasets. Displayed above each FU map are: the number of FUs, the number of connecting lines between FUs, and the relative number of connecting lines (between parentheses). A circle with a cross inside indicates the geographic center of all Voronoi centers belonging to an FU and has a corresponding gray value.*

responds to the coloring of a plane graph, assigning different colors to adjacent vertices. Humans can perceive about five different colors rapidly and accurately [Hea96], whereas there can be more than five FUs. However, for any plane graph, four colors are sufficient [RSST96].

To find a four-coloring of the FUs, the FUs are sorted by their number of neighboring FUs, from high to low. From a set of four available colors, each FU is assigned (one by one) a color different from its neighbors. If there are already four different colors among its neighbors, there is an impasse. To solve the impasse, we make use of a *c-d* Kempe chain, which is a connected component of a colored graph with vertices colored c or d. Interchanging the two colors in a Kempe chain is referred to as Kempe chaining [MS91]. This is executed randomly with neighbors of the impasse FU, until the impasse is solved. If this does not terminate within a certain number of attempts, then the FUs are sorted randomly before restarting the coloring procedure.

In an FU map, FUs below a certain size may be omitted. Instead of four different colors, four different gray levels are used here (Fig. 2, left, middle).

5.5. FU Map Connections

Given the FUs, we define the *inter-FU coherence* c' at frequency λ between two functional units W_1 and W_2 as the sum of the coherence values between one vertex in W_1 and the other vertex in W_2, scaled by the total number of edges between W_1 and W_2:

$$c'_\lambda(W_1,W_2) = \frac{\sum_{i,j}\{c_\lambda(v_i,v_j) \mid v_i \in W_1, v_j \in W_2\}}{|W_1| \cdot |W_2|}. \quad (3)$$

Here, $|W_i|$ indicates the number of vertices in W_i. Note that coherences between any pair of vertices are taken into account, to normalize for the size of the FUs.

A line is drawn between FU centers if the corresponding inter-FU coherence exceeds a threshold. We consistently choose this threshold to be equal to the significance thresh-

old (Eqn. 1), because we already used this threshold to determine the initial graph.

From the FU maps, the number of FUs k and the number of connecting lines m can be deduced. To compare the number of connecting lines across FU maps with varying numbers of FUs, the relative number of connecting lines r is computed as the actual number of connecting lines divided by the possible number of connecting lines, given the number of FUs: $r = \frac{2m}{k(k-1)}$.

6. Results

FU maps including small FUs fail to give a good overview (Fig. 2, left). Therefore, we choose to consider only FUs larger than 5 cells.

In Fig. 3, FU maps are shown for the three datasets. The top row shows FU maps for the EEG frequency band 1-3 Hz, the bottom row for 13-20 Hz. We observe that each FU map shows less clutter than a straightforward data-driven graph visualization without any adaptations (compare Fig. 3 with Fig. 1, left).

In the FU maps (Fig. 3), for each dataset the number of FUs does not differ much between the two EEG frequency bands (compare top with bottom row). The (relative) number of connecting lines is always higher for the low EEG frequency band. This indicates simultaneous activity at a more global scale for a lower EEG frequency and at a more local scale for a higher EEG frequency, in accordance with [NSW*97]. Furthermore, there is a connecting line between a large anterior and a large posterior FU for each of the datasets and for both EEG frequency bands. This is possibly associated with the two most important sources of brain activity for this type of data, located anteriorly (known as P3a) and posteriorly (known as P3b) [CP99, EvWvdN*03].

7. Discussion and Conclusions

EEG coherence analysis is the study of coherence between functional units. Most current analyses use hypothesis-driven regions of interest (ROIs). Existing data-driven graph visualizations for EEG coherence commonly visualize vertices representing electrodes as dots and coherences as edges, resulting in clutter for high-density EEG with up to 512 electrodes. However, without a hypothesis, all coherences should be considered. Therefore, we have developed a new data-driven visualization method for high-density EEG coherence, which strongly reduces clutter and is referred to as functional unit (FU) map. An FU is a spatially connected set of electrodes recording pairwise significantly coherent signals, represented in the graph by a spatially connected clique. In an FU map, the spatial relationship between cells representing electrodes is preserved, and all cells in one FU are assigned an identical color. Adjacent FUs are visualized with different colors and FUs are connected by a line if the average coherence between FUs exceeds a threshold.

FU maps are shown for three datasets containing responses to target stimuli, and for two EEG frequency bands. Comparable conventional findings are rare, because conventional data-driven high-density EEG coherence analysis is cumbersome. However, we find that the (relative) number of connecting lines between FUs is lower for a higher EEG frequency, in accordance with [NSW*97]. Furthermore, connections between anterior and posterior FUs are possibly associated with the two most important sources of brain activity for this data type [CP99, EvWvdN*03].

The method employs two thresholds; one threshold affects the configuration of the FUs, the other the number of connecting lines between FUs. In this paper, both thresholds are chosen equal to the significance threshold for the coherence calculation (Eqn. 1). However, the thresholds may be chosen different from each other. An interactive adaptation of both thresholds will allow a user to manipulate the FUs and the connecting lines, while maintaining a data-driven visualization. Additionally, the minimum FU size can be adapted interactively, thereby simultaneously affecting the number of connecting lines.

Conventional analysis of high-density EEG coherence is typically based on the selection of a small number of electrodes as markers. Each marker is supposed to be representative for all other electrodes in a certain ROI. Traditionally, the selection of these markers is hypothesis-driven. In our approach, FU maps can be used for a data-driven selection of markers: the number of markers, their location, and their region of influence can be derived directly from an FU map. In other words, FU maps can be used as a preprocessing step for conventional analysis.

In EEG research, several datasets are usually compared in a so-called group analysis. Although FU maps vary from dataset to dataset, there are solutions. Visually, multiple FU maps can be compared when displayed next to each other. Analytically, FU maps can be compared on the basis of their (underlying) graph structure, e.g., using (inexact) graph matching, which computes a similarity value between two graphs [BA83].

The FU map based on Voronoi-connected maximal clique detection is also suitable for the visualization of other similarity measures for signals recorded by spatially distributed sensors.

References

[BA83] BUNKE H., ALLERMANN G.: Inexact graph matching for structural pattern recognition. *Pattern Recognition Letters 1* (1983), 245–253. 7

[BK73] BRON C., KERBOSCH J.: Algorithm 457: finding all cliques of an undirected graph. *Commun. ACM 16*, 9 (1973), 575–577. 2, 4, 5

[CJM03] CHIRICOTA Y., JOURDAN F., MELANCON G.:

Software components capture using graph clustering. In *Proc. 11th IEEE International Workshop on Program Comprehension* (2003), p. 217. 3

[CP99] COMERCHERO M. D., POLICH J.: P3a and P3b from typical auditory and visual stimuli. *Clin. Neurophysiol. 110*, 1 (1999), 24–30. 7

[DMFTS02] DELORME A., MAKEIG S., FABRE-THORPE M., SEJNOWSKI T.: From single-trial EEG to brain area dynamics. *Neurocomputing 44–46* (2002), 1057–1064. 1, 3

[EvWvdN*03] ELTING J. W., VAN WEERDEN T. W., VAN DER NAALT J., DE KEYSER J. H. A., MAURITS N. M.: P300 component identification using source analysis techniques: Reduced latency variability. *Journal of Clinical Neurophysiology 20*, 1 (2003), 26–34. 7

[FR91] FRUCHTERMAN T. M. J., REINGOLD E. M.: Graph drawing by force-directed placement. *Software - Practice and Experience 21*, 11 (1991), 1129–1164. 1, 3

[GLdJ06] GLADWIN T. E., LINDSEN J. P., DE JONG R.: Pre-stimulus EEG effects related to response speed, task switching and upcoming response hand. *Biol. Psychol. 72*, 1 (2006), 15–34. 2, 3

[Hea96] HEALEY C. G.: Choosing effective colours for data visualization. In *Proc. IEEE Visualization* (1996), pp. 263–270. 5

[HF77] HOLSHEIMER J., FEENSTRA B. W.: Volume conduction and EEG measurements within the brain: a quantitative approach to the influence of electrical spread on the linear relationship of activity measured at different locations. *Electroencephalogr. Clin. Neurophysiol. 43*, 1 (1977), 52–58. 1, 2, 4

[HMM00] HERMAN I., MARSHALL M. S., MELANCON G.: Density functions for visual attributes and effective partitioning in graph visualization. In *Proc. IEEE Symposium on Information Vizualization* (Washington, DC, USA, 2000), IEEE Computer Society, p. 49. 1, 3

[HRA*95] HALLIDAY D. M., ROSENBERG J. R., AMJAD A. M., BREEZE P., CONWAY B. A., FARMER S. F.: A framework for the analysis of mixed time series/point process data - theory and application to the study of physiological tremor, single motor unit discharges and electromyograms. *Progress in Biophysics and Molecular Biology 64*, 2/3 (1995), 237–278. 2

[Jun99] JUNGNICKEL D.: *Graphs, Networks and Algorithms*. Springer, 1999. 2

[KBS97] KAMIŃSKI M., BLINOWSKA K., SZELENBERGER W.: Topographic analysis of coherence and propagation of EEG activity during sleep and wakefulness. *Electroencephalography and Clinical Neurophysiology 102* (1997), 216–227. 1, 2, 3

[LRMV99] LACHAUX J. P., RODRIGUEZ E., MARTINERIE J., VARELA F. J.: Measuring phase synchrony in brain signals. *Human Brain Mapping 8*, 4 (1999), 194–208. 1

[MS91] MORGENSTERN C. A., SHAPIRO H. D.: Heuristics for rapidly four-coloring large planar graphs. *Algorithmica 6* (1991), 869–891. 6

[MSvdHdJ06] MAURITS N. M., SCHEERINGA R., VAN DER HOEVEN J. H., DE JONG R.: EEG coherence obtained from an auditory oddball task increases with age. *J. Clin. Neurophysiol. 23*, 5 (2006), 395–403. 1, 3

[NSW*97] NUNEZ P. L., SRINIVASAN R., WESTDORP A. F., WIJESINGHE R. S., TUCKER D. M., SILBERSTEIN R. B., CADUSCH P. J.: EEG coherency. I: Statistics, reference electrode, volume conduction, Laplacians, cortical imaging, and interpretation at multiple scales. *Electroencephalogr. Clin. Neurophysiol. 103*, 5 (1997), 499–515. 3, 7

[RSST96] ROBERTSON N., SANDERS D. P., SEYMOUR P., THOMAS R.: A new proof of the four-color theorem. *Electron. Res. Announce. Amer. Math. Soc. 2*, 1 (1996), 17–25. 5

[Sri99] SRINIVASAN R.: Methods to improve the spatial resulution of EEG. *International Journal of Bioelectromagnetism 1*, 1 (1999). 3

[SRSP99] STEIN A. V., RAPPELSBERGER P., SARNTHEIN J., PETSCHE H.: Synchronization between temporal and parietal cortex during multimodal object processing in man. *Cerebral Cortex 9* (1999), 137–150. 1, 3

[tCMR05] TEN CAAT M., MAURITS N. M., ROERDINK J. B. T. M.: Tiled parallel coordinates for the visualization of time-varying multichannel EEG data. In *EuroVis, Symposium on Data Visualization (Eurographics/IEEE VGTC)* (2005), pp. 61–68. 1

[tCMR07] TEN CAAT M., MAURITS N. M., ROERDINK J. B. T. M.: Design and evaluation of tiled parallel coordinate visualization of multichannel EEG data. *IEEE Transactions on Visualization and Computer Graphics 13*, 1 (2007), 70–79. 1

[TTT06] TOMITA E., TANAKA A., TAKAHASHI H.: The worst-case time complexity for generating all maximal cliques and computational experiments. *Theor. Comput. Sci. 363*, 1 (2006), 28–42. 5

[Vor08] VORONOI G.: Nouvelles applications des paramètres continus à la théorie des formes quadratiques, deuxième memoire, recherche sur les parallellèdres primitifs. *Journal für die Reine und Angewandte Mathematik 134* (1908), 198–287. 2, 3

[WCG03] WONG N., CARPENDALE S., GREENBERG S.: EdgeLens: An interactive method for managing edge congestion in graphs. In *Proc. IEEE Symposium on Information Visualization* (2003), pp. 51–58. 1, 3